

See discussions, stats, and author profiles for this publication at: <https://www.researchgate.net/publication/256836072>

Brazilwood Reds: The (Photo)Chemistry of Brazilin and Brazilein

ARTICLE *in* THE JOURNAL OF PHYSICAL CHEMISTRY A · SEPTEMBER 2013

Impact Factor: 2.69 · DOI: 10.1021/jp404789f · Source: PubMed

CITATION

1

READS

103

6 AUTHORS, INCLUDING:



J. Sérgio Seixas de Melo

University of Coimbra

161 PUBLICATIONS 3,601 CITATIONS

SEE PROFILE



João Pina

University of Coimbra

59 PUBLICATIONS 1,010 CITATIONS

SEE PROFILE



Tatiana Vitorino

New University of Lisbon and Italian National ...

5 PUBLICATIONS 12 CITATIONS

SEE PROFILE



A. Jorge Parola

New University of Lisbon

119 PUBLICATIONS 1,829 CITATIONS

SEE PROFILE

Brazilwood Reds: The (Photo)Chemistry of Brazilin and Brazilein

Raquel Rondão,[†] J. Sérgio Seixas de Melo,^{*,†} João Pina,[†] Maria J. Melo,^{‡,§} Tatiana Vitorino,[‡] and A. Jorge Parola[‡][†]Department of Chemistry, University of Coimbra, P3004-535 Coimbra, Portugal[‡]Requimte, CQFB, Departamento de Química, FCT - Universidade Nova de Lisboa, 2829-516 Caparica, Portugal[§]Requimte, Departamento de Conservação e Restauro, Universidade Nova de Lisboa, 2829-516 Caparica, Portugal

S Supporting Information

ABSTRACT: The ground and excited state (in the singlet state, S_1) acid–base equilibria, together with the photophysical properties of the two main constituents of brazilwood, brazilin and brazilein, have been investigated in aqueous solutions in the pH range: $-1 < \text{pH} < 10$. Brazilin is the colorless reduced form of brazilein where three ground and three excited state species ($B_{\text{red}}H_n$, with $n = 2-4$ representing the protonated hydroxyl groups) are observed with two corresponding acidity constants: $\text{p}K_{a1} = 6.6$ and $\text{p}K_{a2} = 9.4$ ($\text{p}K_{a1}^* = 4.7$ and $\text{p}K_{a2}^* = 9.9$, obtained from the Förster cycle). In the case of brazilein, three ground species ($\text{p}K_{a1} = 6.5$ and $\text{p}K_{a2} = 9.5$) and four excited state species were identified (again from the Förster cycle: $\text{p}K_{a1}^* = 3.9$ and $\text{p}K_{a2}^* = 9.8$). The colorless species (brazilin) presents a high fluorescence quantum yield ($\phi_F = 0.33$) and competitive radiative channel ($k_F = 1.3 \times 10^9 \text{ s}^{-1}$) over radiationless processes ($k_{NR} = 2.6 \times 10^9 \text{ s}^{-1}$). In contrast to this behavior, brazilein displays a ϕ_F value 2 orders of magnitude lower and a dominance of the radiationless decay pathways, which is suggested to be linked to an excited state proton transfer leading to a quinoidal-like structure. This is further supported by time-resolved data (obtained in a ps time domain). The overall data indicates that brazilin is more prone to degradation than brazilein, mainly due to the high efficiency of the radiationless decay channel (likely through internal conversion), which confers a stabilizing inherent characteristic to the latter. In the case of brazilein, the efficiency of the radiationless channel is linked to an excited state intramolecular proton transfer resulting from an excited state equilibrium involving neutral and zwitterionic tautomeric species of this compound. Furthermore, a theoretical study has been performed with the determination of the optimized ground-state and excited molecular geometries for the two compounds together with the prediction of the lowest vertical one-electron excitation energy and the relevant molecular orbital contours and charge densities changes using density functional theory calculations. These were found to corroborate differences in acidity in the ground and excited states.



■ INTRODUCTION

In the early Middle Ages, brazilwood, an important source for pink and bright reddish-purple colors, began to be imported into Europe from Sri Lanka, India, and Southeast Asia.^{1,2} These redwoods, known as *brazil*, *bresil*, *brasiliun*, *verzi*, or *verzino* (among other variations), and later brazilwood, became widely available in European markets by the 14–15th centuries and were used for textile dyeing and inks as well as to prepare lake pigments (dye-metal complexes) for manuscript illumination, particularly in the precious *Books of Hours*.^{1–4} At that time, the Asian sappanwood, *Caesalpinia sappan*, was the only brazilwood species known as such.¹ However, the discovery of South America in the beginning of the 16th century, by the Portuguese, introduced new species similar to sappanwood, from which the same main chromophore brazilin/brazilein could be extracted.⁵ The main brazilwood species from both Asia and America are *Caesalpinia sappan*, *Caesalpinia echinata*, *Caesalpinia brasiliensis*, *Caesalpinia violacea*, *Caesalpinia crista*, and *Haematoxylum brasiletto*.^{1,6,7} These started to be imported to Europe replacing the Asian sappanwood. Some are still important today, not so much as a source of red dye, but for the

medicinal properties of their components (*C. sappan*) or because their wood is considered ideal for making violin bows (*C. echinata*).¹

Brazilin is the major compound isolated from *Caesalpinia sp.*, which, upon exposure to air and light, forms the deep red brazilein (Scheme 1). This exposure oxidizes the hydroxyl group in C9 to a quinoid moiety as well as C12. It is the π -electron delocalization made available by these oxidations that further extends the overall π -conjugated system that gives rise to the characteristic deep red color of brazilwood.

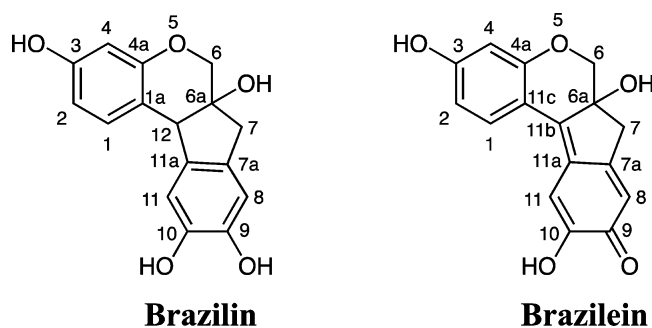
The first report of the isolation of brazilin was made by Chevreul in 1808 (quoted in refs 8 and 9), but its empirical formula was only disclosed in 1864 (quoted in refs 8 and 9), when Bolley, as the result of several analyses, suggested the formula $C_{22}H_{20}O_7$. Ten years later, Lybermann and Burg proposed the correct $C_{16}H_{14}O_5$ formula.^{8,9}

Received: May 15, 2013

Revised: September 18, 2013

Published: September 19, 2013

Scheme 1. Structures of the Major Component in Brazilwood, Colorless Brazilin, and Its Oxidized and Colored Form, Brazilein



The study of the degradation pathways of colorants is of fundamental interest since it provides critical information about the artists aesthetic perspective, conceptions, and choices, and how the work has changed over time. The processes taking place in the excited state, after absorption of light by a molecule, are usually complex, and in heterogeneous systems, such as the ones offered by works of art, they are still a challenge.^{10–12} This may explain why so few systematic studies have been carried out and published for historic molecules that have been used by man in artistic production, namely, to create works of art.^{11,13} In order to measure and predict color changes in brazilwood dyes and pigments, both photochemistry and photophysical studies are mandatory for a better assessment of conservation condition and to envisage the best preservation strategies of artworks such as, for example, the *Books of Hours* or Van Gogh paintings.^{13,14} In this work, a comprehensive analysis of the acid–base equilibria, photophysics and photochemistry of both brazilin and brazilein is, to the best of our knowledge, performed for the first time.

EXPERIMENTAL SECTION

Brazilin Isolation. Adapting a procedure described by Kim et al.,¹⁵ 100 g of Brazilwood chips (from Kremer pigments) were placed in a 1 L beaker with 500 mL of methanol and left there for two days during which time the mixture was occasionally stirred. The liquid became dark red, and the mixture was filtrated; the procedure was repeated twice. The extract was concentrated under reduced pressure and partitioned in H₂O–MeOH (3:1, total volume of 200 mL) and ethyl acetate (100 mL × 3). A small part of the obtained extract was redissolved in methanol and further chromatographed in a silica gel column using as eluent a mixture of CHCl₃/MeOH (from 15:1 to 5:1). The first eluted fractions were collected and reduced to dryness. Some of the portions were dissolved in water and acidified with 0.1 M HCl and further injected in an HPLC–DAD using the separation method reported in ref 16. The NMR spectra of the purified brazilin were obtained and compared with those in refs 5, 17, and 18; despite this purification brazilin shows the presence of a residual amount of brazilein.

Brazilein Isolation. Brazilein was easily isolated by following the procedure described by Berger,⁵ which will be briefly summarized; 300 g of chips were allowed to stand in 1700 mL of methanol for three days. The mixture was filtrated and concentrated under vacuum (bath temperature: 45 °C) to a volume of 100 mL, which was then allowed to stand for four days. The black crystals of brazilein that precipitated were

filtered off by suction, washed with ice-cold methanol, and dried under a vacuum. The latter procedure was repeated twice yielding a total of 900 mg of brazilein, whose purity was confirmed by ¹H NMR and HPLC–DAD. The NMR spectrum of the isolated brazilein was in agreement with that published in the literature.^{15,17,18}

Characterization and Studies in Solution. For photophysical studies, mother solutions of brazilin and brazilein were prepared by dissolving the dyes in 1 mL of methanol, after which this solution was dropped into a 20 mL volumetric balloon, and acidified water (0.1 M HCl) was added. The pH of the solutions was adjusted by addition of HCl, NaOH, or universal buffer of Theorell and Stenhagen.¹⁹ The universal buffer used was prepared in the following way: 2.3 mL of 85% (w/w) phosphoric acid, 7.00 g of monohydrated citric acid, and 3.54 g of boric acid were dissolved in water; 343 mL of 1 M NaOH was then added, and the solution was diluted to 1 dm³ with water.

UV–vis spectra were acquired with a Shimadzu UV-2100 spectrometer. The molar extinction coefficients, ϵ , were obtained from the slope of the plot of the absorption versus the concentration using (at least) six solutions of different concentrations (correlation values >0.999).

Fluorescence measurements were recorded with a Horiba-Jobin-Yvon Fluorolog 3–2.2 spectrometer. Fluorescence spectra were corrected for the wavelength response of the system.

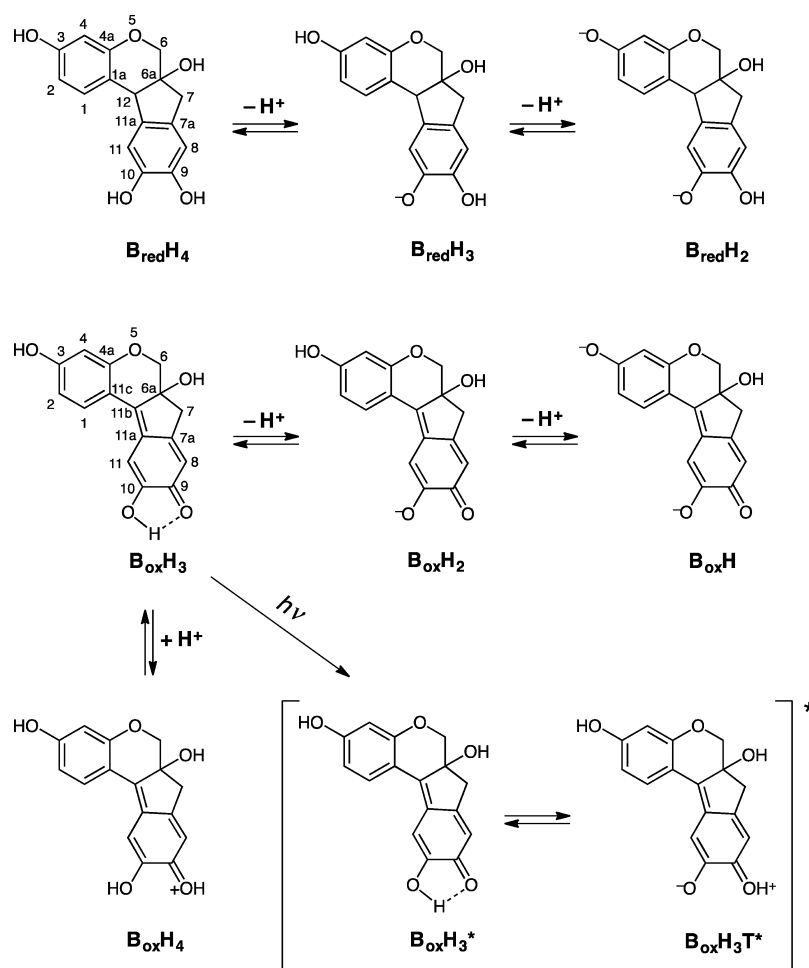
Room temperature fluorescence quantum yields (ϕ_F) were determined by comparison with standards of known quantum yield. The emission quantum yields of these reference compounds should be independent of the excitation wavelength, so the standards can be used in their full absorption range. In practice, the quantum yields are determined by comparison of the integrated area under the emission spectra of optically matched solutions of the samples ($\int I(\lambda)^{cp} d\lambda$) and that of the suitable reference compound ($\int I(\lambda)^{ref} d\lambda$). The absorption and emission range of the samples (cp) and reference (ref) compound should match as much as possible. The absorbance values should be kept as low as possible to avoid inner filter effects (usually with $A < 0.2$). In these conditions, using the same excitation wavelength, the unknown fluorescence quantum yield (ϕ_F^{cp}) is calculated using eq 1,²⁰

$$\phi_F^{cp} = \frac{\int I(\lambda)^{cp} d\lambda}{\int I(\lambda)^{ref} d\lambda} \cdot \frac{OD_{ref}}{OD_{cp}} \cdot \frac{n_{cp}^2}{n_{ref}^2} \cdot \phi_F^{ref} \quad (1)$$

where n_x is the refractive index of the solvents in which the compounds and the reference were respectively dissolved and OD_x is the optical density of the reference (ref) and compound (cp) at the excitation wavelength. The fluorescence standards (references) used were rubrene ($\phi_F = 0.27$ in methanol²¹) for brazilein and naphthalene ($\phi_F = 0.2$ in cyclohexane²¹) for brazilin.

Fluorescence decays were measured using a home-built TCSPC apparatus. In this apparatus, the excitation source consists of a picosecond Spectra Physics mode-lock Tsunami laser (Ti:Sapphire) model 3950 (repetition rate of about 82 MHz, tuning range 700–1000 nm), pumped by a Millennia Pro-10s, frequency-doubled continuous wave (CW), diode pumped, solid-state laser ($\lambda_{em} = 532$ nm). A harmonic generator model GWU-23PS (Spectra Physics) is used to produce the second and third harmonic from the Ti:Sapphire laser exciting beam frequency output. For brazilin, the samples

Scheme 2. Acid–Base Equilibria of Brazilin ($B_{red}H_n$) and Brazilein ($B_{ox}H_n$) and Formation of Brazilein Tautomers in the Excited State^a



^aNumbering is given for the fully protonated forms. It should be noticed that the order of deprotonation on the hydroxyl group in positions 3 and 10, both in brazilin and brazilein, is arbitrary, although theory seems to confirm the order presented in this scheme; see text for more details.

were measured with excitation at 282 nm. Fluorescence decays and the instrumental response function (IRF) were collected using 1024 channels in a 0.8 ps per channel scale, until 1×10^3 counts at maximum were reached. The full width at half-maximum of the IRF (measured using a LUDOX scattering solution in water) was about 22 ps and was highly reproducible with identical system parameters. After deconvolution of the experimental signal, the time resolution of the apparatus is ca. 3 ps.²² Further details about the equipment are elsewhere described.²² The fluorescence decays were analyzed using the modulating functions method of Striker.²³

In the case of brazilein, the fluorescence decays of the compounds were obtained using a PicoQuant Picoled (model LDH-P-C-450b, $\lambda_{exc} = 451$ nm with a repetition rate of 40 MHz) as the excitation source. In this case the full width at half maximum of the IRF was about 75 ps and was highly reproducible with identical system parameters.

¹H NMR spectra were run on a Bruker AMX 400 instrument operating at 400.13 MHz (¹H). For brazilin, deuterated acetone was used as solvent, while for brazilein, for a better comparison with ref 15, deuterated DMSO was used.

The ground state molecular geometry was optimized using the density functional theory (DFT) by means of the Gaussian 03 program,²⁴ under B3LYP/6-31G** level.^{25,26} Optimal

geometries were determined on isolated entities in a vacuum, and no conformational restrictions were imposed. For the resulting optimized geometries, time-dependent DFT calculations (using the same functional and basis set as those in the previously calculations) were performed to predict the vertical electronic excitation energies. The excited-state geometry was optimized using the Hartree–Fock based single-excitation restricted configuration interaction (RCIS)²⁷ method with the 3-21G* basis set. Molecular orbital contours were plotted using Molekel 5.4.

The excited-state geometries were optimized using the Hartree–Fock based single excitation restricted configuration interaction (RCIS)²⁷ method with the 3-21G* basis set.

RESULTS

Solution Behavior, pH Dependence. Brazilin and brazilein were titrated in aqueous solution in a batch procedure through pH jumps carried out from a mother solution at pH = 1 (0.1 M HCl) to higher pH values (up to ~12). In order to easily identify the species in equilibrium, the acronyms $B_{red}H_n$ for brazilin (where n stands for the number of protonated hydroxyl groups) and $B_{ox}H_n$ for brazilein are proposed, Scheme 2. As mentioned in the Experimental Section, brazilin has been exhaustively purified. However, it still presents a residual

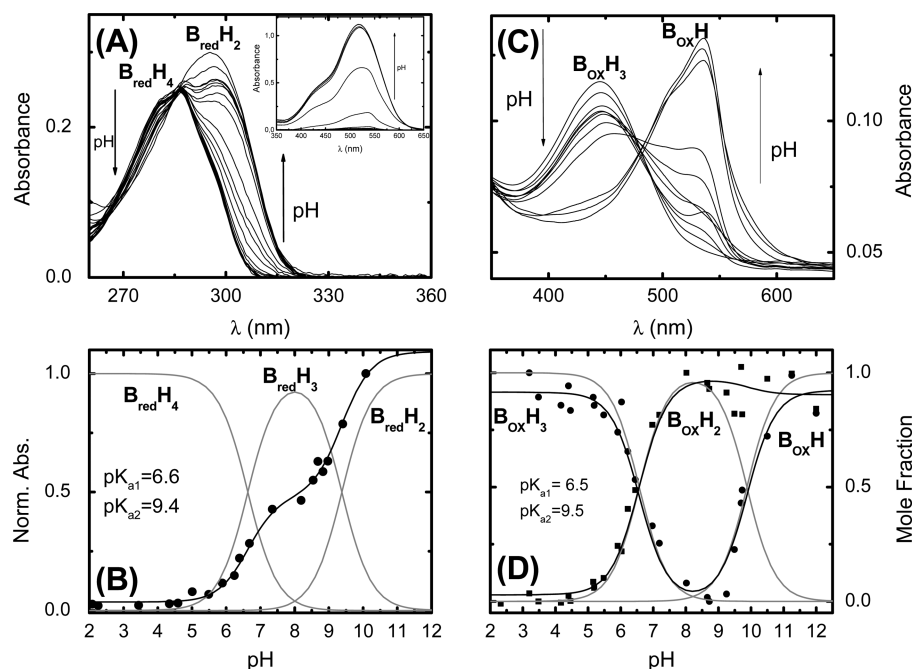


Figure 1. (A) Spectral variations occurred upon pH jumps from an equilibrated aqueous solution of brazilin at pH = 1 to higher pH values. (B) Calculated pK_a values upon fitting of the absorbance at 295 nm (black line), and mole fraction distribution of the species (gray line). (C) Spectral variations occurred upon pH jumps from an equilibrated solution of brazilin at pH = 1 to higher pH values. (D) Calculated pK_a values resulting from the fitting of the absorbance at 450 and 550 nm (black line), and mole fraction distribution of the species (gray line). The inset in A results from the increase in absorption for pH > 9 (see text for more details).

amount of brazilin, which most likely results from a small degree of oxidation induced by oxygen (dissolved in the solvent, even though this has been purged/bubbled with N_2 or Ar) and light.

The titration curves were built by plotting the change in absorbance at different pH values and are depicted in Figure 1.

For brazilin, it was observed that for pH > 10, the solutions become first deep red (a large increase in the absorption maximum as a result of a full deprotonation of brazilin), that is followed by a fading (the solution eventually becomes colorless), Figure 2.

Spectral and Photophysical Data. Figure 3 presents the absorption, fluorescence emission, and excitation spectra of

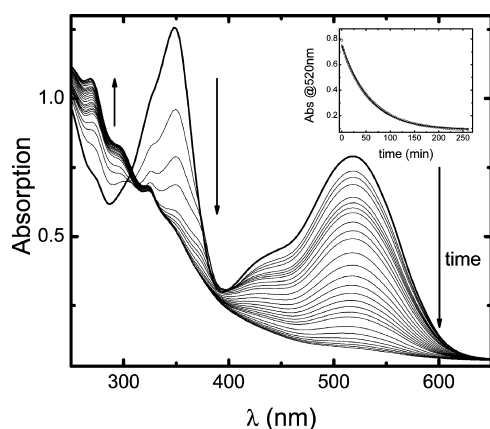


Figure 2. Spectral changes observed upon a pH jump from an equilibrated solution of brazilin at pH = 1 to pH = 12. As inset, the plot for the absorption change with time obtained at 520 nm, $T = 293$ K, fitted as a monoexponential decay, with a fading constant of 0.0175 min^{-1} .

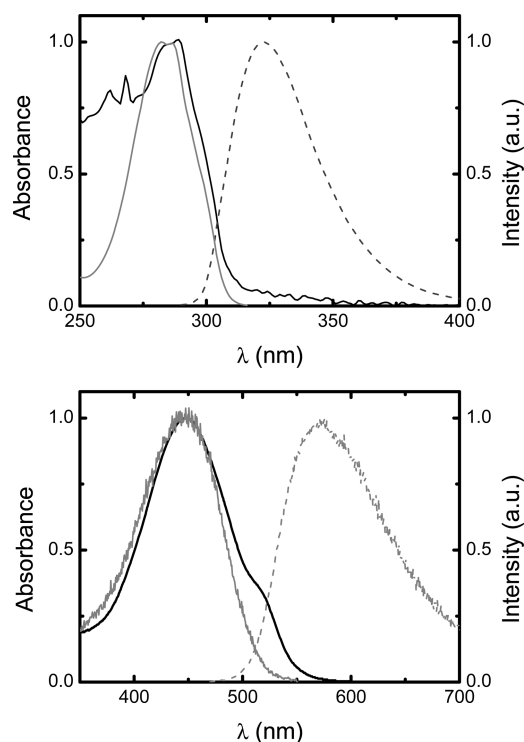


Figure 3. Absorption (black line) and fluorescence emission (dotted gray line) and excitation (gray line) spectra of brazilin (top panel) and brazilin (bottom panel) in 0.1 M HCl, $T = 293$ K.

brazilin at pH ≈ 1 and brazilin at pH ≈ 1.5 , i.e., of the totally protonated $B_{red}H_4$ and $B_{ox}H_3$ species. It is worth emphasizing that there is an almost perfect match between the absorption and fluorescence excitation spectra, which further attests the

Table 1. Spectral (Wavelength Absorption, $\lambda_{\text{max}}^{\text{Abs}}$, and Fluorescence Maxima, $\lambda_{\text{max}}^{\text{Fluo}}$, Molar Extinction Coefficient, ϵ_{ss}) and Photophysical (Stokes Shift, Δ_{ss} , Fluorescence Quantum Yield, ϕ_{F} , Fluorescence Lifetime, τ_{F} , and Radiative, k_{F} , and Radiationless, k_{NR} , Rate Constants) Data for Brazilin at pH = 1 ($\text{B}_{\text{red}}\text{H}_4$ species), and Brazilein at pH = 1.5 ($\text{B}_{\text{ox}}\text{H}_3$), $T = 293 \text{ K}$

	$\lambda_{\text{max}}^{\text{Abs}}$ (nm)	$\lambda_{\text{max}}^{\text{Fluo}}$ (nm)	ϵ_{ss} ($\text{M}^{-1} \text{ cm}^{-1}$)	Δ_{ss} (nm)	ϕ_{F}	τ_{F} (ps)	k_{F} (ns^{-1})	k_{NR} (ns^{-1})
brazilin ($\text{B}_{\text{red}}\text{H}_4$)	286	323	6160	37	0.330	260	1.27	2.58
brazilein ($\text{B}_{\text{ox}}\text{H}_3$)	448	570	4680	122	0.0068	100 ^a	0.068	9.93

^aMajor component of a biexponential decay; however, at pH = −1 the decay is single exponential with a decay time value of 3.89 ns; see text for further details.

purity of the investigated species; this is of utmost relevance for the subsequent photophysical studies.

Table 1 presents the spectral and photophysical data for brazilin at pH = 1 ($\text{B}_{\text{red}}\text{H}_4$ species), and brazilein at pH = 1.5 ($\text{B}_{\text{ox}}\text{H}_3$).

Steady-State Fluorescence Dependence with pH for Brazilin and Brazilein. The fluorescence titration curve for brazilin, exciting at the isosbestic point ($\lambda_{\text{exc}} = 290 \text{ nm}$), is depicted in Figure 4.

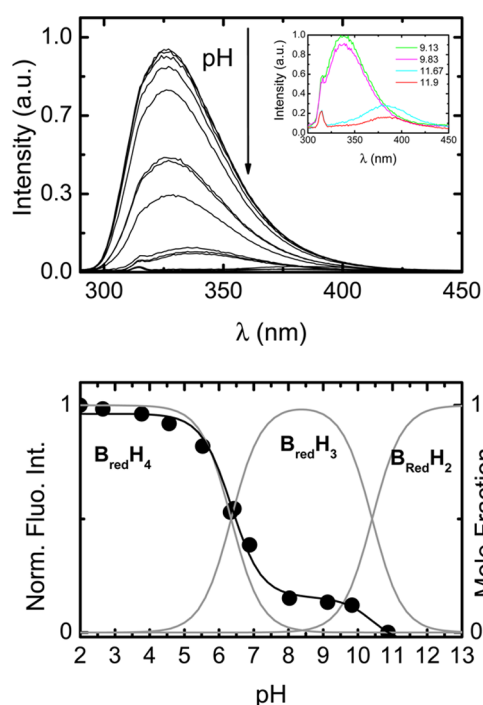


Figure 4. Top: spectral variations occurred upon a pH jump from equilibrated solutions of brazilin at pH 1 to higher pH values. Bottom: mole fraction distribution of the species (gray line) as a function of pH from which an apparent $\text{pK}_{\text{a}}^* = 6.3$ resulting from the fitting of the emission at 350 nm (black line) is obtained; as is discussed in the text this value is overestimated, and a more satisfactory value is obtained from the Förster cycle. Shown as inset in the top figure is a magnified view of the spectra between 9.13 and 11.9 showing the additional band at ~400 nm; see text for more details.

For the $\text{B}_{\text{red}}\text{H}_4^*$ species (pH = 1), a fluorescence band with emission maximum at 323 nm is observed. Upon going to higher pH values, the fluorescence emission gradually decreases, and a very weak band at ~400 nm begins to appear at pH > 11 (see Figure 4), which is identified with the emission of the $\text{B}_{\text{red}}\text{H}_2^*$ species.

For brazilein, due to the solution's fading (for pH > 10), the emission spectra were collected immediately after solution preparation (after a pH jump from an equilibrated solution of

brazilein at pH = 1) at $\lambda_{\text{exc}} = 480 \text{ nm}$ (isosbestic point in Figure 1C). The obtained fluorescence emission spectra after pH jumps in the range 1–12 are shown in Figure 5. From the spectra, it can be observed that from pH = 1.4 to pH = 7.6 the fluorescence intensity increases, and for higher pH values it decreases sharply. From the dependence of the fluorescence intensity with the pH, two apparent pK_{a}^* can be obtained. However, as will be shown in the Discussion section, more satisfactory estimates of the excited state pK_{a} values, pK_{a}^* , are obtained through the thermodynamic Förster cycle.

Time-Resolved Fluorescence Dependence with pH for Brazilin. The variation of the time-resolved fluorescence decays with the pH was also investigated. This was obtained with pH jumps from a stock solution of brazilin at pH = 1.

From the pre-exponential dependence with pH, a titration curve could be constructed (similar to that obtained from the steady-state data in Figure 1), from which a $\text{pK}_{\text{a}} = 6.3$ is obtained; see Figure 6.

DISCUSSION

Solution Behavior: pH Dependence. From Figure 1A) it can be seen that for brazilin, upon an increase in pH up to pH ≤ 10 a small increase in the absorption of the ~280 nm band is observed together with (for pH > 10) the appearance of an absorption band with maximum at ~500 nm (see inset of Figure 1). The first process, occurring for pH < 10, corresponds to the deprotonation of brazilin with two measurable pK_{a} values: $\text{pK}_{\text{a}1} = 6.6$ and $\text{pK}_{\text{a}2} = 9.4$; see Scheme 2. At very acidic pH values (~1), a single (and dominant) species exists with an absorption maximum at 286 nm; upon increasing the pH a new band (with $\lambda_{\text{max}} = 295 \text{ nm}$) gradually appears. The second process, associated with the appearance of the 500 nm band (see Figure 3), should correspond to the third deprotonation of brazilin followed by fast oxidation to fully deprotonated brazilein. This is further confirmed by the appearance of the same band around 520 nm upon titration of brazilein.

The spectral changes presented by brazilein after pH jumps from equilibrated stock solutions at pH = 1 are depicted in Figure 1C from which two pK_{a} values could be determined: $\text{pK}_{\text{a}1} = 6.5$ and $\text{pK}_{\text{a}2} = 9.5$. This shows that oxidation (of C12 and of the hydroxyl group in C9) of brazilin to yield brazilein leads to minor changes on the pK_{a} values (pK_{a} values of 6.6 and 9.4 for brazilin).

The fading of brazilein, reported in Figure 2, has been previously described for haematein (extracted from logwood and chemically related to the structure of brazilein).²⁸ The color fading of the fully deprotonated form of brazilein is likely to arise from a degradation process involving the breakdown of the carbon skeleton (discontinuation of the π -conjugation), as suggested by the increase in absorption in the UV region, concomitantly with the decrease in absorption in the visible region. Moreover, the diminishing of the 520 nm band with

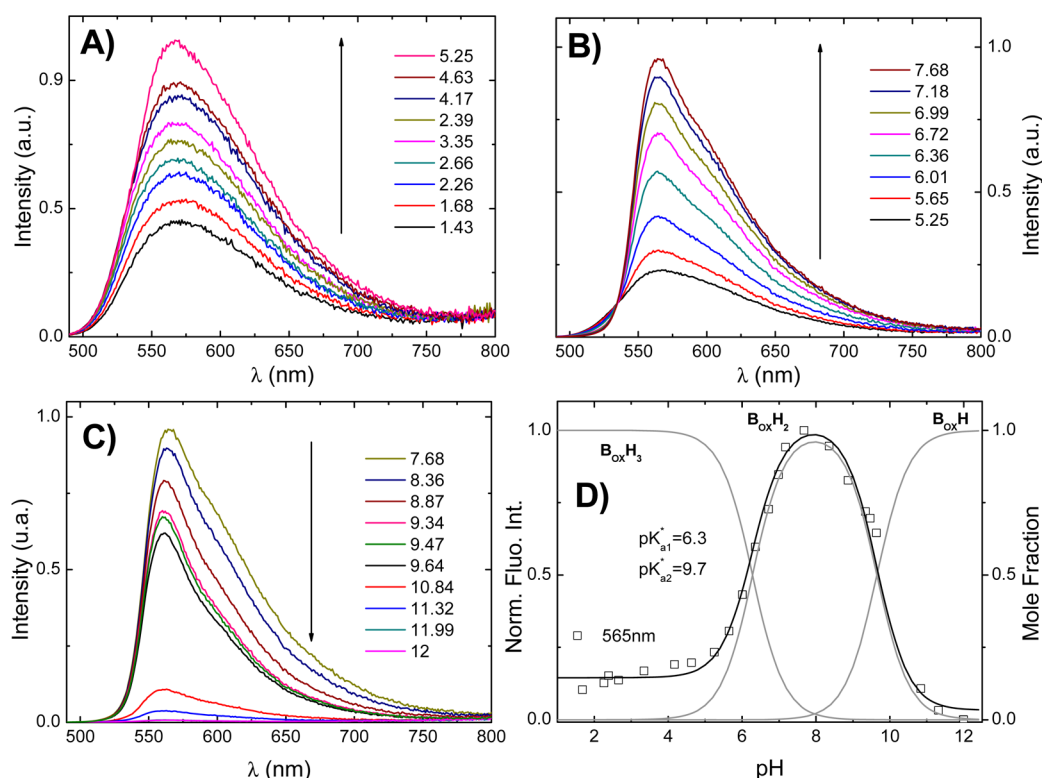


Figure 5. Fluorescence spectral variations ($\lambda_{exc} = 480$ nm) observed upon pH jumps from an equilibrated solution of brazilin at pH = 1 to 1.43 < pH < 5.25 (A), 5.25 < pH < 7.68 (B), and 7.68 < pH < 12 (C). (D) Apparent pK_a^* values obtained upon fitting of the emission at 565 nm (black line) and mole fraction distribution of the species (gray line). As is discussed in the text, more satisfactory estimates of the pK_a^* values are obtained from the thermodynamic Förster cycle.

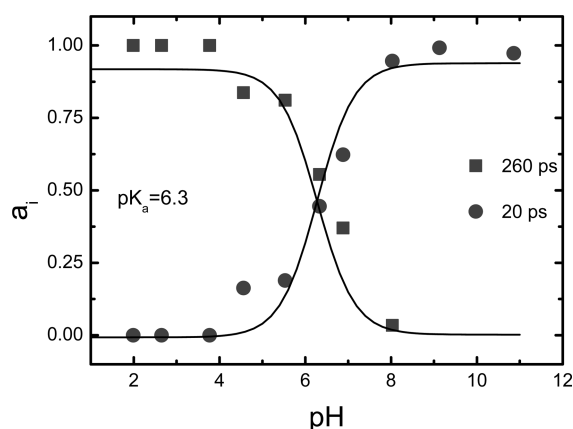


Figure 6. Plot of pre-exponential coefficients (a_i) associated to brazilin decay times of 20 and 260 ps as a function of the pH (after pH jumps from a stock solution in 0.1 M HCl), collected at $\lambda_{em} = 325$ nm and with excitation at $\lambda_{exc} = 282$ nm, $T = 293$ K.

time follows a clear single exponential decay law, with a time constant of 0.0175 min^{-1} .

Spectral and Photophysical data for Brazilin. Table 1 presents the spectral and photophysical properties of brazilin at pH = 1 ($B_{red}H_4$ species) and brazilin at pH = 1.5 ($B_{ox}H_3$).

The obtained fluorescence lifetime is single exponential (see Figure S11 in Supporting Information) reinforcing the idea that at lower pH values the $B_{red}H_4$ brazilin species is dominant; see Table 1.

From the fluorescence titration curves, a $pK_{a1}^* = 6.3$ was obtained presumably corresponding to the $B_{red}H_4^* \rightarrow B_{red}H_3^*$

equilibria in the excited state; however, as discussed elsewhere, in situations where only one of the species of the acid–base pair is fluorescent (in the present case better equated as associated to a single band) the dependence of fluorescence on pH does not, in general, yield the excited state equilibrium constant.^{29,30} Estimates for the pK_a^* values were therefore obtained from the thermodynamic Förster cycle,³¹ through eq 2.^{32,33}

$$pK_a^* = pK_a + \frac{E_A - E_{HA}}{2.303RT} \quad (2)$$

where E_A and E_{HA} stand for the energies of the unprotonated and protonated species in equilibrium, respectively. These values were obtained through the interception of the normalized absorption and emission spectra of each species. The temperature considered was $T = 293.15$ K. As others have previously discussed, the various uncertainties in the determination of pK_a^* and solvent effects (particularly sensitive in highly acidic solutions) should limit these determinations to the range $0 < \text{pH} < 14$.^{29,30} Accordingly, we have obtained (eq 2), the following pK_a^* values for brazilin ($pK_{a1}^* = 4.7$ and $pK_{a2}^* = 9.9$; this last for the second $B_{red}H_3^* \rightarrow B_{red}H_2^*$ equilibrium) and brazilin ($pK_{a1}^* = 3.9$, $pK_{a2}^* = 9.8$). From these values, two observations are worth noting. The first is the fact that — as found in other phenolic-like compounds — the two compounds are more acidic in the first excited singlet state than they are in the ground state; the second is that as a result of the close proximity in shape and maxima of the $B_{red}H_3/B_{red}H_2$ and $B_{ox}H_2/B_{ox}H$, the values of the second deprotonation rate constant are approximately identical in both the ground and excited states, which suggests that upon abstraction of the

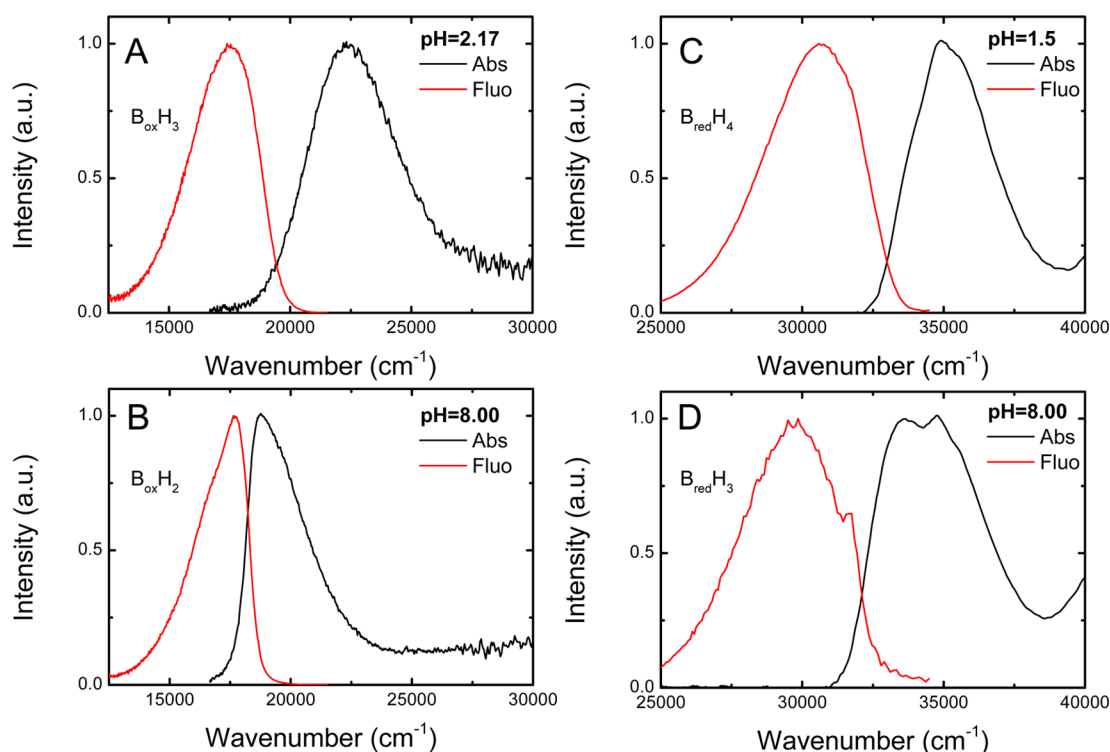


Figure 7. Absorption and fluorescence spectra for the (A) $B_{ox}H_3$ (pH = 2.17) and (B) $B_{ox}H_2$ (pH = 8.0) forms of brazilin and (C) $B_{red}H_4$ (pH = 1.5) and (D) $B_{red}H_3$ (pH = 8.0) forms of brazilin, plotted as a function of the wavenumber.

first proton, abstraction of a second one does not introduce significant perturbation in the charge distribution difference between the ground and excited states. Indeed, this can further be seen from the relatively high Stokes shift (Δ_{ss}) in the case of the first deprotonation equilibria (in agreement with other aromatic-like structures, e.g., β -naphthol, hydroxycoumarins,^{34,35} where a unique hydroxyl group exists, and therefore a single pK_a^* , and there is a clear change in the charge distribution between the ground and first excited singlet states) leading to very significant changes between the pK_a and pK_a^* values (see Figure 7A,C) in contrast with the situation of the second pK_a^* , where the Stokes shift is largely decreased; see Figure 7B,D.

It is also worth commenting on the radiative and radiationless rate constants of the $B_{red}H_4$ species of brazilin. As can be observed from Table 1, in spite of the significant fluorescence quantum yield value (0.330 in Table 1), the k_F and k_{NR} values are of the same order of magnitude. This indicates that both deactivation channels of the excited state are operative. The high stability of historic dyes such as indigo^{36,37} and mauveine³⁸ has been linked to a high and efficient deactivation of the S_1 state through the internal conversion deactivation channel. In order to investigate which radiationless process is more dominant with brazilin ($S_1 \sim \sim \rightarrow S_0$ internal conversion or the $S_1 \sim \sim \rightarrow T_1$ intersystem crossing), laser flash photolysis experiments have been carried out in order to obtain the transient triplet–triplet absorption spectra and therefore to characterize the triplet state of this molecule. However, even at low laser energy doses, photochemistry took place (conversion of brazilin into brazilin; see Supporting Information). This has made it impossible to obtain the triplet quantum yield for brazilin.

From the time-resolved data of brazilin, it can be seen that at very acidic pH values (pH \approx 1; see Figure S1, Supporting

Information), the fully protonated $B_{red}H_4$ species is the only species present, and the fluorescence decay is single-exponential; see Figure S1. However, the gradual increase of the pH leads to deprotonation of brazilin, and at pH \approx 4 (where both $B_{red}H_4^*$ and $B_{red}H_3^*$ are present; see Figure 3B) a second component begins to appear leading to biexponential decays (with decay components of 20 and 260 ps) until pH \approx 9. Moreover, it is also interesting to note that the decay time values were found constant all over the pH range, with values of 20 and 260 ps, whereas the associated pre-exponential factors vary reciprocally as illustrated in Figure 4. At pH \geq 9, the fluorescence decays are now almost single exponential, the dominant decay time value being 20 ps (attributed to the $B_{red}H_3$ species and also a contribution of the $B_{red}H_2$). Also at pH 9 and above, the dominant species are the $B_{red}H_3^*$ the $B_{red}H_2^*$ forms of brazilin with a decay time of 20 ps. This means that either the $B_{red}H_2^*$ excited species cannot be differentiated from the $B_{red}H_3^*$ or that its decay time value is below our time resolution (\sim 3 ps).

Spectral and Photophysical Data for Brazilin. The spectral and photophysical properties of the fully protonated form of brazilin obtained at pH \approx 1.5 ($B_{ox}H_3$) are summarized in Table 1. Comparison with data for brazilin shows that brazilin absorption and fluorescence spectra are strongly red-shifted relative to the former. Moreover, and in contrast with brazilin's fully protonated form ($B_{red}H_4$), the Stokes shift value is now very significant for brazilin's $B_{ox}H_3$ form; see Figure 7. Additionally, the fluorescence quantum yield value of brazilin is found to be 2 orders of magnitude lower than that of brazilin; see Table 1.

Also from Table 1 it is clear — and again in contrast with brazilin — that the radiationless dominates over the radiative deactivation pathways. This, together with the pronounced Stokes shift, strongly suggests the presence of additional

processes in the first excited singlet state of brazilin. Indeed, when investigating the time-resolved behavior of brazilin, and in contrast to brazilin, where at pH = 1 ($B_{\text{red}}H_4$ fully protonated species) the decay was found to be single exponential, for brazilin ($B_{\text{ox}}H_3$) the decay is now biexponential.

Further observation of Figure 5D also indicates that it is likely that additional equilibrium at pH below 4 may be present. Therefore, an attempt to obtain the lifetime of the totally protonated species was made at pH values below 1, by dissolving brazilin in a (commercial) concentrated solution of perchloric acid ($HClO_4$), pH ≈ -1 . A value of 3.89 ns was found for pH ≈ -1 ; see Figure 8. This is further supported from theoretical calculations as will be discussed below.

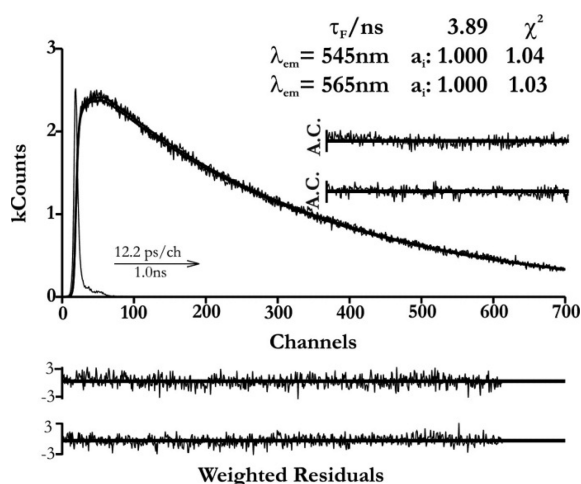


Figure 8. Fluorescence decay of brazilin in aqueous solution at pH ≈ -1 , with excitation at 460 nm, and collected at 545 and 565 nm and $T = 293$ K. Shown as insets are the decay times (τ /ns), pre-exponential factors (a_i), and chi-squared values (χ^2). Also shown are the weighted residuals for a better judgment of the quality of the fits.

Measuring the decays for pH > -1 shows, however, that this decay time strongly decreases with increasing pH and the decays become bi- and triexponential. Indeed, between pH 3 and 4, the decays are biexponential with values of 0.35 and 0.11 ns. Figure 9 shows the dependence with the pH of the major decay time component. Because of the solution fading (which

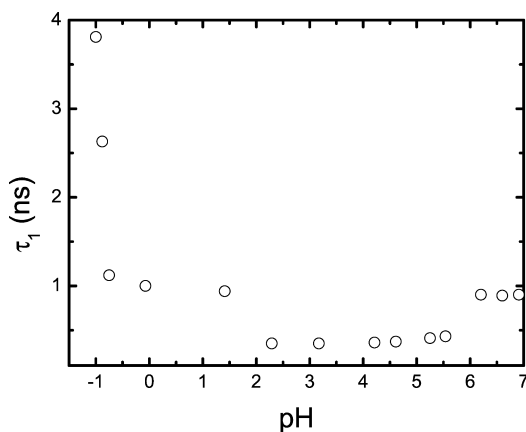


Figure 9. Dependence with pH of the decay time associated to the major decay component for brazilin; $\lambda_{\text{exc}} = 450$ nm, and $\lambda_{\text{em}} = 565$ nm, $T = 293$ K.

starts at pH ≈ 7), we were unable to obtain fluorescence decays above this pH value. These combined data suggest that an additional and efficient radiationless pathway is present in brazilin above pH ≈ 0 .

Brazilin contains an *o*-hydroxyquinone moiety that is expected to stabilize its neutral form, $B_{\text{ox}}H_3$, through an intramolecular hydrogen bond between the carbonyl oxygen at C9 and the hydroxyl hydrogen at C10, Scheme 2. This provides a very efficient excited state intramolecular proton transfer (ESIPT) with the establishment of an excited state equilibrium between the neutral $B_{\text{ox}}H_3^*$ and the zwitterionic $B_{\text{ox}}H_3T^*$ tautomeric species.^{39,40} This decay channel at acidic pH values competes with fluorescence, promoting a strong decrease of the fluorescence intensity for pH ≥ 0 (see Figure 10), concomitant

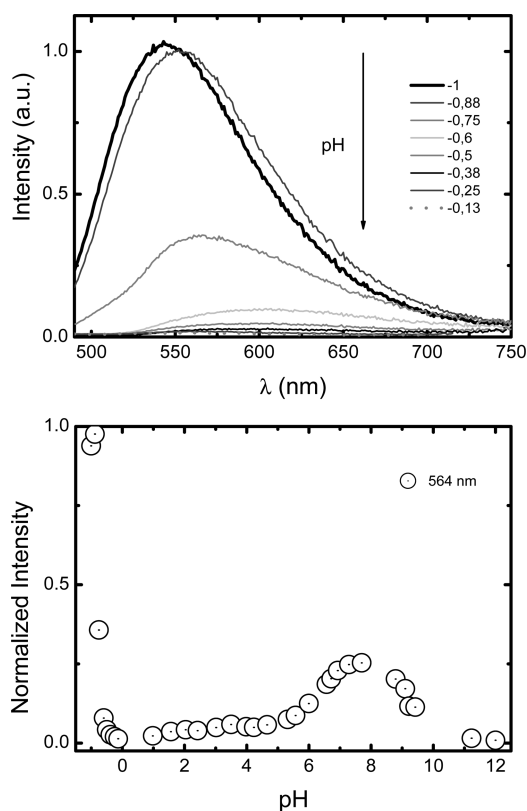


Figure 10. Fluorescence emission from aqueous solutions of brazilin, from pH ≈ -1 to pH ≈ 0 , $\lambda_{\text{exc}} = 480$ nm, $T = 293$ K (top) and plot of the respective fluorescence intensity at 564 nm (bottom); data for pH ≥ 0 was taken from Figure 5.

with the observed strong decrease in the decay times (from 3.89 to 0.1 ns; see Figures 8 and 9 and Figure S2 in Supporting Information). It also explains the observed biexponential decays in the range $1 < \text{pH} < 4$. At extremely acidic pH values, the intramolecular hydrogen bond in $B_{\text{ox}}H_3$ is destroyed due to the protonation of the carbonyl oxygen. On the other hand, the solvent ability for intermolecular brazilin-to-water proton transfer should be strongly reduced due to the high proton concentration. The fluorescence emission at pH ≈ -1 is thus due to the cationic $B_{\text{ox}}H_4$ species (see Scheme 2), which apparently is stable at this pH and not prone to excited state proton transfer (ESPT). The observation of the emission spectra at the pH ≈ -1 shows a blue shift of the fluorescence wavelength maximum ($\lambda_{\text{max}} = 543$ nm for pH ≈ -1 and $\lambda_{\text{max}} =$

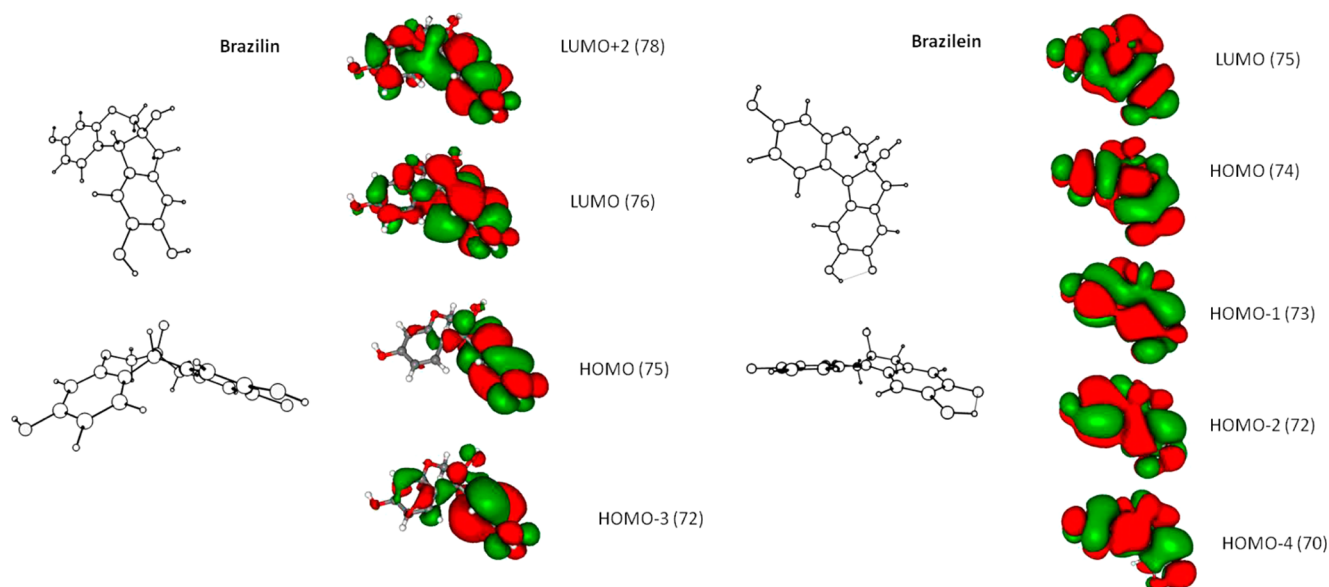


Figure 11. DFT//B3LYP/6-31G** optimized ground-state geometry together with the MO energy levels and the MO contours for brazilin and brazilein. The structures presented at the left of the MO contours of brazilin and brazilein are for the same ground-state geometry and represent only two different projection/views of the same structure. Dihedral angles are given in the text.

564 nm for $\text{pH} \geq 1$) that is compatible with an emission originated from this new species.

Theoretical Calculations. Figure 11 depicts the ground-state optimized geometry structures together with the pertinent HOMO (HOMO- X , with $X = 0, 1, 2$, and 4 for brazilein and $X = 0$ and 3 for brazilin) and LUMO (LUMO + Y , $Y = 0$ and $+2$ for brazilin and $Y = 0$ for brazilein) energy levels and their molecular orbital (MO) contours for brazilin and brazilein obtained at the DFT//B3LYP/6-31G** level. For brazilin, a singlet–singlet transition is predicted at 256.77 nm with an oscillator strength (f) of 0.1067, essentially with contributions of transitions involving the MO $72 \rightarrow 78$ and $75 \rightarrow 76$, whereas in the case of brazilein a singlet–singlet transition at 419.65 nm with $f = 0.4826$ is predicted involving transitions with contributions from the MO $70 \rightarrow 75$, $72 \rightarrow 75$, $73 \rightarrow 75$ and $74 \rightarrow 75$.

A more in-depth analysis of this data reveals the following. There is a clear departure from the overall planarity of brazilin with a dihedral angle of 28.2° ($\text{C1}–\text{C1a}–\text{C12}–\text{C11a}$; see numbering in Scheme 2) relative to brazilein with a dihedral angle of 22.3° ($\text{C1}–\text{C11c}–\text{C11b}–\text{C11a}$). Moreover, with brazilin the HOMO is clearly more localized (essentially in one-half of the structure, $\text{C6a}–\text{C12}–\text{C11}–\text{C10}–\text{C9}–\text{C8}–\text{C7a}–\text{C7}$), whereas in the LUMO (and LUMO+2) the electron density is now also delocalized in the other moiety of the molecule, which suggests that a charge-transfer character is likely to be associated to this transition. In the case of brazilein, the HOMO and LUMO MO contours, associated with the lowest singlet–singlet energy transition, are clearly delocalized through the entire backbone. These observations are in line with the more delocalized nature of the MO in brazilein relative to brazilin. Moreover, theory also shows an increase in charge density (here obtained as the absolute value of the Mulliken atomic charges) upon going from the ground to the excited state. In the case of brazilin with values of 0.19032 for the oxygen in the hydroxyl group connected to C10 (for numbering, see Schemes 1 and 2), 0.183893 for the oxygen connected to C3 and 0.168159 for the oxygen connected to C9.

Although not in an absolute way, these data seem to support the idea that the deprotonation will follow the order C10, C3, C9. In the case of brazilein, the values are 0.183453 for the oxygen of the hydroxyl group connected to C3 and 0.199304 for the oxygen of the hydroxyl group connected to C10, again giving support to the order of deprotonation indicated in Scheme 2.

CONCLUSIONS

A comprehensive investigation on the acid–base and excited state characteristics of brazilin and brazilein has been undertaken for the first time. The radiative and radiationless decay channels in brazilin were found to have similar contributions to the deactivation of this molecule, contrasting with brazilein where the radiationless channel was found dominant. Differences have been found for both brazilein and brazilin in the ground and first excited pK_a values with more acidic $\text{B}_{\text{ox}}\text{H}_3$ and $\text{B}_{\text{red}}\text{H}_4$ species in the excited state. For brazilein, evidence has been given supporting the existence of an excited state proton transfer. Furthermore, the results from TDF calculations give support to the differences in the pK_a values in the ground and excited states and to the different nature of the $\text{S}_0 \rightarrow \text{S}_1$ transition in the two compounds. Also it was observed that at alkaline pH values, brazilein displays a gradual disappearance of its red color with time. Taking into account that brazilwood lake pigments were used to create the pink color characteristic of the *Books of Hours* created in French workshops during the 15th century, this finding brings new insights into the rationale of the preparation of medieval lake pigments as described in contemporary treatises or recipe books and the role played by aluminum ion. It is possible that the fading process observed at alkaline pH (finished within $\sim 3–4$ h) is overcome in the presence of aluminum ion, which binds to the dye producing the lake pigment, precluding the deprotonation of brazilein. This will be further investigated.

■ ASSOCIATED CONTENT

■ Supporting Information

Additional fluorescence decays of brazilin in 0.1 M HCl, at $T = 293$ K, with excitation at 282 nm and of brazilein in 0.1 M HCl, at $T = 293$ K, with excitation at 450 nm. This material is available free of charge via the Internet from <http://pubs.acs.org>.

■ AUTHOR INFORMATION

Corresponding Author

*E-mail: sseixas@ci.uc.pt.

Notes

The authors declare no competing financial interest.

■ ACKNOWLEDGMENTS

We are grateful to POCI (project PTDC/QUI-QUI/099388/2008), FCT and FEDER/COMPETE for further funding. R.R. acknowledges FCT for a Ph.D. grant (SFRH/BD/38882/2007), and T.V. a BI grant under Project PTDC/EAT-EAT/104930/2008. Finally, we thank REQUIMTE supporting project PEst-C/EQB/LA0006/2011 and CQC supporting project PEst-C/QUI/UI0313/2011.

■ REFERENCES

- (1) Cardon, D. *Natural Dyes: Sources, Tradition, Technology and Science*; Archetype Publications: London, 2007.
- (2) Melo, M. J. History of Natural Dyes in the Ancient Mediterranean World. In *Handbook of Natural Colorants*, Bechtold, T.; Mussak, R., Eds.; John Wiley & Sons, Ltd: New York, 2009; p 20.
- (3) Roger, P.; Villela-Petit, I.; Vandroy, S. The Brasil Colorants in Illuminated Manuscripts from the Middle Ages - Recomposition Based on Ancient Formulations. *Stud. Conserv.* **2003**, *48*, 155–170.
- (4) Kirby, J. Red Lake Pigments: Sources and Characterisation. In *Fatto d'Archimbia – Los Pigmentos Artificiales en las Técnicas Pictóricas*; del Egido, M.; Kroustallis, S., Eds.; Ministerio de Educación, Cultura y Deporte: Madrid, 2012; pp 157–170.
- (5) Berger, S.; Sicker, D. *Classics in Spectroscopy: Isolation and Structure Elucidation of Natural Products*; Wiley-VCH: New York, 2009; p 211–230.
- (6) Nowik, W. The Possibility of Differentiation and Identification of Red and Blue 'Soluble' Dyewoods: Determination of Species used in Dyeing and Chemistry of their Dyestuffs. In *Dyes in History and Archaeology*; Kirby, J., Ed.; Archetype Publications Ltd: Lyons/Greenwich, U.K., 2001; Vol. 16/17, pp 129–144.
- (7) Perkin, A. G.; Everest, A. E. *The Natural Organic Colouring Matters*; Longmans, Green & Co: London, 1918.
- (8) Gilbody, A. W.; Perkin, W. H.; Yates, J. Brazilin and Haematoxylin Part I. *J. Chem. Soc.* **1901**, *79*, 1396–1411.
- (9) Robinson, R. Chemistry of Brazilin and Haematoxylin. *Bull. Soc. Chim. Fr.* **1958**, *1*, 125–134.
- (10) Grazia, C.; Clementi, C.; Miliani, C.; Romani, A. Photophysical Properties of Alizarin and Purpurin Al(III) Complexes in Solution and in Solid State. *Photochem. Photobiol. Sci.* **2011**, *10*, 1249–1254.
- (11) Romani, A.; Clementi, C.; Miliani, C.; Favaro, G. Fluorescence Spectroscopy: A Powerful Technique for the Noninvasive Characterization of Artwork. *Acc. Chem. Res.* **2010**, *43*, 837–846.
- (12) Miliani, C.; Daveri, A.; Spaabaek, L.; Romani, A.; Manuali, V.; Sgamellotti, A.; Brunetti, B. G. Bleaching of Red Lake Paints in Encaustic Mummy Portraits. *Appl. Phys. A: Mater. Sci. Process.* **2010**, *100*, 703–711.
- (13) Claro, A.; Melo, M. J.; Seixas de Melo, J. S.; van den Berg, K. J.; Burnstock, A.; Montague, M.; Newman, R. Identification of Red Colorants in Van Gogh Paintings and Ancient Andean Textiles by Microspectrofluorimetry. *J. Cult. Herit.* **2010**, *11*, 27–34.
- (14) Nieder, E.; Hendriks, E.; Burnstock, A. Colour Change in Sample Reconstructions of Vincent van Gogh's Grounds due to Wax-Resin Lining. *Stud. Conserv.* **2011**, *56*, 94–103.
- (15) Kim, D. S.; Baek, N. I.; Oh, S. R.; Jung, K. Y.; Lee, I. S.; Lee, H. K. NMR Assignment of Brazilein. *Phytochemistry* **1997**, *46*, 177–178.
- (16) Melo, M. J.; Sousa, M.; Parola, A. J.; Seixas de Melo, J. S.; Catarino, F.; Marcalo, J.; Pina, F. Identification of 7,4'-Dihydroxy-5-methoxyflavylium in "Dragon's blood": To Be or Not To Be an Anthocyanin. *Chem.—Eur. J.* **2007**, *13*, 1417–1422.
- (17) Fuke, C.; Yamahara, J.; Shimokawa, T.; Kinjo, J.; Tomimatsu, T.; Nohara, T. 2 Aromatic-Compounds Related to Brazilin from *Caesalpinia-Sappan*. *Phytochemistry* **1985**, *24*, 2403–2405.
- (18) Huang, Y. D.; Zhang, J. S.; Pettus, T. R. R. Synthesis of (\pm)-Brazilin using IBX. *Org. Lett.* **2005**, *7*, 5841–5844.
- (19) Küster, F. W.; Thiel, A. *Tabelle per le Analisi Chimiche e Chimico-Fisiche*, 12th ed.; Hoepli: Milano, 1982.
- (20) Murov, S.; Charnichael, I.; Hug, G. L. *Handbook of Photochemistry*; M. Dekker Inc.: New York, 1993.
- (21) Montalti, M.; Credi, A.; Prodi, L.; Gandolfi, M. T. *Handbook of Photochemistry*, 3rd ed.; CRC Press: Boca Raton, 2006.
- (22) Pina, J.; Seixas de Melo, J.; Burrows, H. D.; Maçanita, A. L.; Galbrecht, F.; Bunnagel, T.; Scherf, U. Alternating Binaphthyl-Thiophene Copolymers: Synthesis, Spectroscopy, and Photophysics and Their Relevance to the Question of Energy Migration versus Conformational Relaxation. *Macromolecules* **2009**, *42*, 1710–1719.
- (23) Striker, G.; Subramaniam, V.; Seidel, C. A. M.; Volkmer, A. Photochromicity And Fluorescence Lifetimes of Green Fluorescent Protein. *J. Phys. Chem. B* **1999**, *103*, 8612–8617.
- (24) Frisch, M. J.; Trucks, G. W.; Schlegel, H. B.; Scuseria, G. E.; Robb, M. A.; Cheeseman, J. R.; Montgomery, J., Jr.; Vreven, T.; Kudin, K. N.; Burant, J. C.; et al. *Gaussian 03*, Revision C.02; Gaussian, Inc.: Wallingford, CT, 2004.
- (25) Becke, A. D. A New Mixing of Hartree-Fock and Local Density-Functional Theories. *J. Chem. Phys.* **1993**, *98*, 1372–1377.
- (26) Francl, M. M.; Pietro, W. J.; Hehre, W. J.; Binkley, J. S.; Gordon, M. S.; Defrees, D. J.; Pople, J. A. Self-Consistent Molecular-Orbital Methods 0.23. A Polarization-Type Basis Set For 2nd-Row Elements. *J. Chem. Phys.* **1982**, *77*, 3654–3665.
- (27) Foresman, J. B.; Headgordon, M.; Pople, J. A.; Frisch, M. J. Toward a Systematic Molecular-Orbital Theory for Excited-States. *J. Phys. Chem.* **1992**, *96*, 135–149.
- (28) Lalor, G. C.; Martin, S. L. Studies on Haematoxylin and Haematein, the Colouring Principles of Logwood 0.2. Behaviour in Aqueous Solutions at Varying pH, and the pK Values. *J. Soc. Dye. Colour* **1959**, *75*, 517–521.
- (29) Lasser, N.; Feitelso, J. Excited-State pK Values From Fluorescence Measurements. *J. Phys. Chem.* **1973**, *77*, 1011–1016.
- (30) Lasser, N.; Feitelson, J. Excited-State pK* Values From Fluorimetry. *J. Phys. Chem.* **1975**, *79*, 1344–1346.
- (31) Förster, T. Die pH-Abhängigkeit Der Fluoreszenz Von Naphthalinderivaten. *Z. Elektrochem.* **1950**, *54*, 531–535.
- (32) Marciniak, B.; Kozubek, H.; Paszyc, S. Estimation of pK_a* in the First Excited Singlet-State - A Physical-Chemistry Experiment that Explores Acid-Base Properties in the Excited-State. *J. Chem. Educ.* **1992**, *69*, 247–249.
- (33) Ireland, J. F.; Wyatt, P. A. H. Acid-Base Properties of Electronically Excited States of Organic Molecules. *Adv. Phys. Org. Chem.* **1976**, *12*, 131–221.
- (34) Laws, W. R.; Brand, L. Analysis of 2-State Excited-State Reactions - Fluorescence Decay of 2-Naphthol. *J. Phys. Chem.* **1979**, *83*, 795–802.
- (35) Seixas de Melo, J. S.; Cabral, C.; Lima, J. C.; Maçanita, A. L. Characterization of the Singlet and Triplet Excited States of 3-Chloro-4-methylumbelliferone. *J. Phys. Chem. A* **2011**, *115*, 8392–8398.
- (36) Seixas de Melo, J.; Moura, A. P.; Melo, M. J. Photophysical and Spectroscopic Studies of Indigo derivatives in their Keto and Leuco Forms. *J. Phys. Chem. A* **2004**, *108*, 6975–6981.

- (37) Seixas de Melo, J. S.; Serpa, C.; Burrows, H. D.; Arnaut, L. G. The triplet State of Indigo. *Angew. Chem., Int. Ed. Engl.* **2007**, *46*, 2094–2096.
- (38) Seixas de Melo, J.; Takato, S.; Sousa, M.; Melo, M. J.; Parola, A. J. Revisiting Perkin's Dyes(s): the Spectroscopy and Photophysics of Two New Mauveine Compounds (B2 and C). *Chem. Commun.* **2007**, 2624–2626.
- (39) Strandjord, A. J. G.; Barbara, P. F. Proton-Transfer Kinetics of 3-Hydroxyflavone - Solvent Effects. *J. Phys. Chem.* **1985**, *89*, 2355–2361.
- (40) Strandjord, A. J. G.; Courtney, S. H.; Friedrich, D. M.; Barbara, P. F. Excited-State Dynamics of 3-Hydroxyflavone. *J. Phys. Chem.* **1983**, *87*, 1125–1133.